HHS Public Access

Author manuscript

J Immunol. Author manuscript; available in PMC 2024 May 01.

Published in final edited form as:

J Immunol. 2023 May 01; 210(9): 1292–1304. doi:10.4049/jimmunol.2200407.

STAT1 controls the functionality of influenza-primed CD4 T cells but therapeutic STAT4 engagement maximizes their antiviral impact

Caroline M. Finn[*], **Kunal Dhume**[*], **Emily Prokop**[*], **Tara M. Strutt**[*], **K. Kai McKinstry, PhD**[*]

[*]Burnett School of Biomedical Sciences, Division of Immunity and Pathogenesis, College of Medicine, University of Central Florida, Orlando, FL, USA

Abstract

It is generally accepted that Influenza A virus infection promotes a Th1-like CD4 T cell response and that this effector program underlies its protective impact. Canonical Th1 polarization requires cytokine-mediated activation of the transcription factors STAT1 and STAT4 that synergize to maximize the induction of the 'master regulator' Th1 transcription factor, T-bet. Here, we determine the individual requirements for these transcription factors in directing the Th1 imprint primed by influenza infection in mice by tracking virus-specific wildtype or T-bet-deficient CD4 T cells in which STAT1 or STAT4 is knocked out. We find that STAT1 is required to protect influenza-primed CD4 T cells from NK cell-mediated deletion and for their expression of hallmark Th1 attributes. STAT1 is also required to prevent type I IFN signals from inhibiting the induction of the Th17 'master regulator', Rorγt, in Th17-prone T-bet$^{-/-}$ cells responding to IAV. In contrast, STAT4 expression does not appreciably impact the phenotypic or functional attributes of wildtype or T-bet$^{-/-}$ CD4 T cell responses. However, cytokine-mediated STAT4 activation in virus-specific CD4 T cells enhances their Th1 identity in a T-bet-dependent manner, indicating that influenza infection does not promote maximal Th1 induction. Finally, we show that the T-bet-dependent protective capacity of CD4 T cell effectors against IAV is optimized by engaging both STAT1 and STAT4 during Th1 priming, with important implications for vaccine strategies aiming to generate T cell immunity.

Introduction

CD4 T cells protect against Influenza A virus (IAV) infection through multiple mechanisms (1, 2). Their importance is seen, for example, through analysis of MHC-II-deficient mice, that lack CD4 T cells and that are marked by delayed IAV clearance compared to WT mice (3), and in studies finding that while WT mice depleted of CD8 T cells can clear sublethal IAV infection, mice depleted of both CD4^{+} and CD8^{+} cells do not survive (4). Furthermore, IAV-specific effector CD4 T cells isolated from mice during primary infection and transferred to naive hosts can protect against an otherwise lethal IAV challenge (5, 6). Indeed, IAV-specific memory CD4 T cells generated through infection or vaccination are

Corresponding author: K. Kai McKinstry, PhD, kai.mckinstry@ucf.edu, Phone: 407-266-7137, Fax: 407-266-7002.

critical components of optimal immunity in mice and humans, especially when preexisting neutralizing antibodies are absent (2, 7–9).

To successfully combat pathogens, CD4 T cells must differentiate into specialized effector subsets that are marked by distinct phenotypic and functional attributes (10). This process is initiated by innate cytokines produced upon infection that promote the expression of so-called ‘master regulator’ transcription factors. While there is heterogeneity within the pool of IAV-primed CD4 T cells (11), the vast majority express hallmarks of the Th1 subset, an effector program that is strongly associated with protection against IAV (12). These include expression of the Th1 ‘master regulator’ T-bet, production of the cytokines IFNγ and TNF, and upregulation of the chemokine receptor CXCR3 which optimizes trafficking of effector cells to the infected lung (13). These and other Th1 attributes are thus widely used to assess CD4 T cell responses in animal and clinical studies focusing on IAV, and viral infection more generally.

We recently showed that T-bet-deficient CD4 T cells still can give rise to effector cells with some Th1 identity during IAV infection (13), and that the transcription factor Eomesodermin (Eomes) is essential to promote these residual Th1 attributes (14). While the regulation of Eomes induction in CD4 T cells is incompletely understood, it has been associated with Th1 programming in some situations (15). This suggests that upstream signaling involved in Th1 induction could be responsible for promoting both T-bet and Eomes expression in CD4 T cells responding to IAV. Interestingly, while very few WT CD4 T cells primed by IAV develop into Th17 cells, some IAV-primed T-bet$^{-/-}$ cells, and even more T-bet$^{-/-}$/Eomes$^{-/-}$ cells, acquire Th17 hallmarks including expression of the Th17 ‘master regulator’, Rorγt, and production of IL-17 and IL-22. This alternative antiviral Th17 programming in CD4 T cells lacking T-bet and Eomes is directed by IL-6 and TGFβ present in the infected lung (14). Whether or not upstream transcriptional regulators of Th1 differentiation constrain Th17 development in T-bet$^{-/-}$ CD4 T cells is unclear, but important to address as highly-polarized Th17 effectors can also protect against IAV (14), and are thus a potential target of vaccination.

STAT1 and STAT4 are critical ‘pioneering’ transcription factors that support the initial phases of Th1 development largely by promoting strong T-bet expression. Activation of STAT1, classically through IFNγ signaling, initiates T-bet activity that is stabilized and further enhanced through STAT4 activation, classically in response to IL-12 (16). These pathways can act independently to promote degrees of Th1 identity in some settings (17), and STAT4 activation can support certain aspects of Th1 programing independently of T-bet (18–20). The extent to which STAT1 activation can promote Th1 programming in the absence of T-bet is not as clear. Furthermore, the relative degree to which the STAT1 and STAT4 pathways in CD4 T cells responding to IAV regulate the development of antiviral CD4 T cell effectors has not been critically assessed. Here, we delineate the individual requirements for STAT1, STAT4, and T-bet expression by CD4 T cells during IAV infection in promoting Th1 identity and protective capacity in WT CD4 T cells. We also determine how STAT1 and STAT4 regulate the Eomes-dependent Th1 attributes as well as the Th17 attributes that develop in T-bet$^{-/-}$ cells primed by IAV. To do so, we tracked virus-specific WT or T-bet$^{-/-}$ CD4 T cells deficient for either STAT1 or STAT4 during primary IAV

infection in otherwise WT mice. This experimental approach focuses on CD4 T cell-intrinsic regulation by STAT1 or STAT4 in the context of a STAT1 and STAT4 replete environment during the infection.

We find that STAT1 expression is required to both protect IAV-primed effector cells from NK cell-mediated deletion and for them to express T-bet-dependent phenotypic and functional Th1 hallmarks at levels comparable to WT IAV-primed effector cells. Unexpectedly, STAT1 is also needed for T-bet$^{-/-}$ cells to develop Th17 responses; its expression is required to prevent a type I IFN (IFNα/β) signaling pathway that restricts Rorγt induction in T-bet$^{-/-}$ CD4 T cells responding in the infected lung. In contrast, STAT4 does not impact the phenotypic or functional attributes of WT or T-bet$^{-/-}$ cells primed by IAV. However, treatment of infected mice with IL-12, which activates STAT4, dramatically enhances the Th1 imprint of WT, but not of T-bet$^{-/-}$ cells. Furthermore, priming WT IAV-specific CD4 T cells *in vitro* with both STAT1- and STAT4-activating cytokines, to maximize their Th1 imprint, promotes effector cells that are better able to protect naive mice against lethal IAV challenge than STAT1$^{-/-}$ and especially STAT4$^{-/-}$ cells primed in the same conditions. Our findings support the concept that vaccines harnessing STAT4 activation to boost Th1 differentiation beyond that induced naturally by infection could significantly improve T cell immunity against IAV.

Materials and Methods

Mice

Naive donor CD4 T cells for adoptive transfer experiments were obtained from 4–8 week old OT-II TcR transgenic mice on either a WT, *Tbx21*$^{-/-}$ (T-bet$^{-/-}$), *Stat4*$^{-/-}$ (STAT4$^{-/-}$), *Stat1*$^{-/-}$ (STAT1$^{-/-}$), *Tbx21*$^{-/-}$/*Stat4*$^{-/-}$ (T/S4$^{-/-}$), or *Tbx21*$^{-/-}$/*Stat1*$^{-/-}$ (T/S1$^{-/-}$) B6 background. The OT-II TcR recognizes aa 323–339 of chicken ovalbumin (OVA). 8–12-week-old WT B6.CD45.1 mice were used as hosts for adoptive transfer experiments. In some experiments mice deficient for expression of IL-12 receptor β chain (IL-12Rβ$^{-/-}$) were used as hosts. WT, STAT1$^{-/-}$, and STAT4$^{-/-}$ B6 mice not on a transgenic background were infected with IAV in some experiments. All mice were originally obtained from Jackson Laboratories (Bar Harbor, ME) and bred at the University of Central Florida. Age- and sex-matched groups of B6.CD45.1 mice were purchased as hosts for adoptive transfer experiments and allowed to acclimatize to conditions in the UCF Lake Nona vivarium for at least 1 week prior to use. All experimental animal procedures were approved by and conducted in accordance with the University of Central Florida's Animal Care and Use Committee's guidelines.

CD4 T cell isolation, effector cultures, and cell transfer

Naive CD4^{+} cells from unmanipulated OT-II donor mice were obtained from pooled spleen and lymph nodes. Single cell suspensions were incubated on nylon wool for one hour followed by Percoll gradient separation to isolate small, resting lymphocytes, and then positive MACS selection using CD4 microbeads (Miltenyi Biotec, Auburn, CA). The resulting cells were routinely > 97% TcR^{+} and expressed a naive phenotype (CD62L^{high},

CD44^{low}). Naive CD4 cells were used to generate effector cells in vitro or in adoptive transfer experiments.

Effector cells were generated as previously described (21) using irradiated T-depleted spleen cells as APC and OVA_{II} peptide. All cultures were supplemented with IL-2 at 11 ng/mL. Th1 culture conditions were further supplemented with anti-IL-4 antibody (Ab) (clone 11B11) at 15 ug/mL and IL-12 at 2 ng/mL. Some cultures were also supplemented with IFNγ at 1000U/ml. Th0 cultures were supplemented with anti-IFNγ Ab (XMG1.2) at 15 ug/mL, anti-IL-4 at 15 ug/mL, and anti-IL-12p40 (C17.8) at 15 ug/mL. Some Th0 cultures were supplemented with IFNα and IFNβ at 100 Units/mL. All blocking antibodies were purchased from BioXcell (West Lebanon, NH). All other reagents were purchased from Peprotech (Rocky Hill, NJ). Effector cultures were fed with fresh media supplemented with IL-2 after 2 days, and the resulting effector cells were analyzed at day 4. If applicable, effectors were thoroughly washed after 4 days, counted, and resuspended prior to adoptive transfer experiments. Naive or effector CD4 cells were adoptively transferred to host mice under light anesthesia in 200μL of RPMI media by retro-orbital injection.

Viral infections and in vivo Ab or cytokine treatments

PR8 and PR8-OVA_{II} (H1N1) were grown in the allantoic cavity of embryonated hen eggs from stocks originally provided by P. Doherty. All viral stocks were characterized at the Trudeau Institute (Saranac Lake, NY). Virus was administered to mice under light isoflurane anesthesia intranasally in 50 μL of PBS. Infected mice were monitored daily for infection-induced morbidity including weight loss, hunched posture, ruffled fur, and reduced movement; mice were euthanized if humane endpoints were reached.

In some experiments NK cells were depleted in mice receiving donor OT-II cells by treatment with 400 μg anti-NK1.1 Ab in 200 μL of PBS (PK136, BioXcell) on −1, 0, 2, 4, 6 dpi by i.p. injection. In other experiments mice received 1 μg of IL-12 (Biolegend; San Diego, CA) in 200 μL of PBS by i.p. injection on 2–6 dpi. Control mice received PBS alone. In other experiments, mice were treated i.p. on days 0, 2, 4, and 6 relative to IAV infection with 250 μg of type I IFN receptor blocking Ab (MAR1-5A3, BioXcell) or with an isotype control (MOPC-21, BioXcell).

Flow cytometry

Single-cell suspensions were washed, resuspended in FACS buffer (PBS plus 0.5% BSA and 0.02% sodium azide) and incubated on ice with 1 μg of anti-FcR (2.4G2) and optimized concentrations of the following fluorochrome-labeled antibodies for surface staining: anti-Thy1.1 (OX-7), anti-Thy1.2 (53-2.1), anti-CD4 (RM4.5), anti-CD45.2, anti-CXCR3 (CXCR3-173), anti-Ly-6C (HK1.4), anti-CD11a (M17/4), anti-MHC class I (8-8-6), and anti-IL-18r (BG/IL18RA).

For intracellular cytokine staining, cells were stimulated for 4 h with 10 ng/ml PMA and 50 ng/ml ionomycin and 10μg/ml Brefeldin A added after 2 h. Cells were then surface stained and fixed for 20 min in 4% paraformaldehyde followed by permeabilization for 10 min by incubation in 0.1% saponin buffer (PBS plus 1% FBS, 0.1% NaN3 and 0.1% saponin). The cells were then stained for cytokine by the addition of fluorescently labeled anti-IFNγ

(XMG1.2), anti-TNF (MP6-XT22), anti-IL-2 (JES6-5H4), anti-IL-17 (TC11-18H10.1), anti-IL-10 (JES5-16E3), or anti-IL-22 (IL22JOP) antibodies for 20 min.

Detection of transcription factors by flow cytometry was conducted using intranuclear staining buffers and fixation as per the manufacture's protocols (ThermoFisher) with fluorescently labeled antibodies against T-bet (Ebio4B10), Rorγt (B2D), and Eomes (Dan11mag). To detect phosphorylated STAT proteins (pSTAT) we used a transcription factor phospho buffer kit (BD Biosciences) as per manufacturer's instructions with an anti-STAT1 pY701 (4a, BD Biosciences) or anti-STAT4 pY693 Ab (38/p-STAT4; BD Biosciences).

All FACS analysis was performed using a BD FACSCanto II (BD Biosciences) or Cytoflex (Beckman Coulter) flow cytometers and FlowJo (Tree Star) analysis software. All antibodies were purchased from BD Biosciences (San Jose, CA), Biolegend (San Diego, CA), or Thermo Fisher (Waltham, MA).

Detection of pulmonary IAV titer

Pulmonary viral titers were determined by quantitation of viral RNA. RNA was prepared from homogenates made from snap-frozen lungs isolated from infected mice using TRIzol (Thermofisher). RNA (2.5 μg) was reverse transcribed into cDNA using random hexamer primers and Superscript II Reverse Transcriptase (Invitrogen). Quantitative PCR was performed to amplify the polymerase (PA) gene of A/PR8-OVA_{II} using a QuantStudio 7 analyzer (Applied Biosystems) with 50 ng of cDNA per reaction and the following primers and probe: forward primer, 5′-CGGTCCAAATTCCTGCTGA-3′; reverse primer, 5′CATTGGGTTCCTTCCATCCA-3′; probe, 5′-6-FAM-CCAAGTCATGAAGGAGAGGGAATACCGCT-3′. Data were analyzed with Sequence Detector (Applied Biosystems). The copy number of the PA gene per 50 ng of cDNA was calculated using a standard curve made with a PA-containing plasmid of known concentration.

Detection of pulmonary cytokines and chemokines

Levels of cytokines and chemokines in lung homogenates collected as described previously (22) were determined using mouse multiplex kits (Millipore) read on a Bio-Plex Multiplex 200 Luminex reader (Bio-Rad), as per manufacturer's instructions.

Statistical analysis

Unpaired, two-tailed, Students *t*-tests, $\alpha = 0.05$, were used to assess whether the means of two normally distributed groups differed significantly. The Welch-correction was applied when variances were found to differ. One-way ANOVA analysis with Bonferroni's multiple comparison post-test was employed to compare multiple means. Significance is indicated as $*P < 0.05$; $**P < 0.005$; $***P < 0.001$; and $****P < 0.0001$. All error bars represent standard deviation.

Results

STAT1 and STAT4 synergize to program Th1 differentiation in vitro

Prior to investigating the transcriptional control of IAV-primed Th1 attributes, we systematically analyzed canonical Th1 development in controlled *in vitro* settings. We first determined how hallmark STAT1-activating (IFNγ) and STAT4-activating (IL-12) cytokines impact the induction of T-bet and Eomes during CD4 T cell priming. To do so, we stimulated naive WT OT-II CD4 T cells with APC and cognate peptide for 4 days in Th1 (supplemented with exogenous IFNγ and IL-12) or Th0 (supplemented with IFNγ- and IL-12-neutralizing Abs) conditions. Th1 but not Th0 priming promoted strong T-bet induction (Fig 1A), as expected. The addition to cultures of either IFNγ or IL-12 alone led to T-bet induction that was about 5-times lower than in full Th1 conditions (Fig 1A). Eomes induction was also maximal in Th1 cultures and was similar in Th0 cultures and in cells primed with IFNγ or IL-12 alone (Supplemental Figure 1). To confirm dependence of the pro-Th1 actions of IFNγ and IL-12 on STAT1 and STAT4, respectively, we next compared T-bet and Eomes expression in cultures of WT, STAT1$^{-/-}$, and STAT4$^{-/-}$ OT-II cells. Exogenous IFNγ promoted T-bet induction in WT and STAT4$^{-/-}$, but not in STAT1$^{-/-}$ cells, when compared to WT Th0 controls (Fig 1B). Similar patterns of expression were seen for Eomes (Supplemental Figure 1). IL-12 alone induced T-bet in WT and STAT1$^{-/-}$, but not STAT4$^{-/-}$ cells (Fig 1C) with little impact on Eomes (Supplemental Figure 1). IFNγ and IL-12 signaling, requiring STAT1 and STAT4, respectively, thus synergize to induce maximal expression of T-bet and Eomes during Th1 priming.

We next asked how STAT1 and STAT4 activation impact the production of Th1-associated cytokines. While more than 90% of WT cells primed in Th1 conditions produced IFNγ after restimulation, this was reduced about 4-fold in STAT1$^{-/-}$ and in STAT4$^{-/-}$ cells (Fig 1D). TNF^{+} cells were also maximal in WT Th1 cultures while STAT1$^{-/-}$ and STAT4$^{-/-}$ Th1 cultures contained more IL-2^{+} cells (Fig 1D). When primed only in the presence of IFNγ, about 30% of WT and STAT4$^{-/-}$ cells, but virtually no STAT1$^{-/-}$ cells, were IFNγ^{+} while TNF^{+} and IL-2^{+} cells were similar across genotypes (Fig 1E). STAT4$^{-/-}$ cells did not produce IFNγ when primed with IL-12 alone, while ~30% of WT but only ~10% of STAT1$^{-/-}$ cells were IFNγ^{+} (Fig 1F). Compromised IFNγ production by STAT1$^{-/-}$ versus WT cells stimulated with IL-12 is perhaps unexpected and suggests a role for STAT1 in maximizing IL-12-driven IFNγ production. Supporting this hypothesis, we detected both STAT1 and STAT4 phosphorylation in WT cells cultured in Th0 conditions for 2 days and then stimulated with IL-12 for 20 minutes (Supplemental Figure 2), a pattern also reported by others (23). The frequencies of TNF^{+} and of IL-2^{+} cells were also lowest in STAT4$^{-/-}$ versus WT and STAT1$^{-/-}$ cells primed with IL-12 alone (Fig 1F). STAT1 and STAT4 activation thus synergize during Th1 priming to promote IFNγ and TNF production, with more IL-2 generally seen from effectors with a weaker Th1 imprint, consistent with T-bet's role as a repressor of *Il2* gene transcription (24).

Altered IAV-induced inflammation in STAT1$^{-/-}$ and STAT4$^{-/-}$ mice impacts WT CD4 T cell responses

We next sought to investigate how the STAT1 and STAT4 pathways impact CD4 T cell effectors generated *in vivo* by IAV infection, which drives a response predominantly characterized by Th1 attributes in WT mice (13). We thus infected WT, STAT1$^{-/-}$, and STAT4$^{-/-}$ mice with a sublethal dose of the mouse-adapted IAV strain, PR8, and analyzed endogenous CD4 T cells in the lungs at 7 days post-infection (dpi). As reported previously (25, 26), numbers of CD44^{high} CD4 T cells were similar between strains (not shown), as were viral titers detected in the lungs at 4 and 7 dpi (Supplemental Figure 3). However, broad analysis of cytokines and chemokines in lung homogenates at 7 dpi revealed higher levels of 19 of 31 analytes in STAT1$^{-/-}$ versus WT mice, while levels of IFNγ, IL-10, IP-10, MIG, and MIP-1β were reduced in the STAT1$^{-/-}$ mice (Supplemental Figure 3). The IAV-induced inflammatory environment in STAT4$^{-/-}$ versus WT mice was more similar, but STAT4$^{-/-}$ mice were marked by reduced levels of IFNγ, IL-10, MIP-1α, and MIP-1β (Supplemental Figure 3).

We reasoned that the altered inflammatory environments in the IAV-primed STAT$^{-/-}$ mice could impact antiviral CD4 T cell responses independently of CD4 T cell-intrinsic STAT expression status. To test this, we transferred CD90.1^{+} WT OT-II cells to WT, STAT1$^{-/-}$, or STAT4$^{-/-}$ mice and challenged them with PR8-OVA$_{II}$, which is recognized by the OT-II TcR (27). While WT donor cell numbers in all hosts were similar at 7 dpi, the frequency of IFNγ^{+} donor cells was reduced in STAT1$^{-/-}$ and STAT4$^{-/-}$ versus WT hosts (Supplemental Figure 3). The WT donor cells in STAT1$^{-/-}$, but not STAT4$^{-/-}$ or WT hosts, also developed IL-17^{+} cells (Supplemental Figure 3). Altered inflammatory environments induced by IAV infection as a result of global STAT1 or STAT4 deficiency can thus impact the priming of Th1 and Th17 attributes in WT anti-viral CD4 T cells.

CD4-intrinsic STAT1 protects activated cells from NK cell attack and supports a Th1 phenotype

To focus on regulation by CD4 T cell-intrinsic STAT1 and STAT4, we transferred WT or STAT-deficient OT-II cells to congenic WT mice and then challenged the mice with PR8-OVA$_{II}$. We first compared WT and STAT1$^{-/-}$ donor cells at 7 dpi. Strikingly, the recovery of STAT1$^{-/-}$ cells was reduced about 5-fold in the spleen and draining lymph node (dLN) versus WT cells, and about 50-times in the lung, reaching limits of detection (Fig 2A). Given that STAT1 signaling has been shown to protect proliferating CD4 T cells from NK cell-mediated killing in other *in vivo* settings (28, 29), we next enumerated STAT1$^{-/-}$ and WT donor cells in host mice treated with NK cell-depleting Ab prior to IAV infection as in our previous studies (30). STAT1$^{-/-}$ donor cells were restored to WT levels in the spleen and dLN by NK cell depletion, but while they were also increased in the lungs, they did not reach WT levels (Fig 2B). Indeed, when compared to WT donors, the STAT1$^{-/-}$ cells expressed lower levels of MHC-I and of the MHC-I-linked molecule Qa-2 in all organs tested (Fig 2C), both of which have been associated with protecting CD4 T cells from NK cell attack *in vivo* (28).

The impaired accumulation of STAT1$^{-/-}$ versus WT effectors in the lungs of NK cell-deficient mice despite similar expansion of both types of donor cells in secondary lymphoid organs mirrors the pattern distinguishing T-bet$^{-/-}$ versus WT CD4 T cell responses against IAV (13). We thus assessed how CD4 T cell-intrinsic STAT1 impacts T-bet expression during IAV infection. We focused on the lungs, the primary site of infection, in NK cell-depleted mice. T-bet was dramatically reduced in STAT1$^{-/-}$ versus WT donor cells. We thus also analyzed T-bet$^{-/-}$ OT-II cells in separate infected NK cell-depleted mice to determine more clearly how STAT1 regulates the expression of T-bet and of T-bet-dependent surface markers expressed by IAV-primed effector CD4 T cells. Using T-bet$^{-/-}$ effector cells as a negative control revealed most WT cells, but only about 20% of STAT1$^{-/-}$ cells, to be T-bet^{+}, with much lower per-cell T-bet expression in STAT1$^{-/-}$ versus WT cells (Fig 2D). In contrast, Eomes, which supports the residual Th1 identity of IAV-primed T-bet$^{-/-}$ cells (14), was increased in T-bet$^{-/-}$ and even more so in STAT1$^{-/-}$ versus WT cells (Fig 2E). We found previously that reduced accumulation of T-bet$^{-/-}$ versus WT cells in the lungs correlated with decreased levels of Ly6C, CXCR3 and CD11a on T-bet$^{-/-}$ effectors (13). These markers were all similarly reduced on STAT1$^{-/-}$ and T-bet$^{-/-}$ versus on WT cells (Fig 2F–H). Together, these results indicate that in addition to protecting IAV-primed CD4 T cells from NK cell-mediated elimination, STAT1 is required for expression of WT levels of T-bet and a T-bet-dependent surface phenotype required for optimal lung homing.

CD4-intrinsic STAT1 is required for maximal Th1 and Th17 function in T-bet$^{-/-}$ CD4 T cells

We next asked how STAT1 impacts Th1 cytokine production by IAV-primed CD4 T cells. Given the similarities between STAT1$^{-/-}$ and T-bet$^{-/-}$ effector phenotypes presented above, and our previous analysis comparing WT and T-bet$^{-/-}$ effectors (13), we present in Figure 3 comparisons of STAT1$^{-/-}$ versus T-bet$^{-/-}$ cells, with average values from WT donor cells from the same experiments included as dotted lines. The recipients of all donor cells were depleted of NK cells to normalize the host environment during IAV infection. Infected mice receiving T-bet$^{-/-}$/STAT1$^{-/-}$ (T/S1$^{-/-}$) cells were also included in the same experiments to determine the extent to which STAT1 expression impacts the cytokine production potential of T-bet$^{-/-}$ CD4 T cells. Indeed, in preliminary experiments we found that IFNγ production by T/S1$^{-/-}$ cells versus T-bet$^{-/-}$ cells primed *in vitro* in Th1 conditions was markedly reduced (Fig 3A), demonstrating robust STAT1-dependent but T-bet-independent priming of Th1 function. Mirroring the pattern seen in STAT1$^{-/-}$ versus WT cells cultured with IL-12, the frequency of IFNγ^{+} T/S1$^{-/-}$ cells was about half that seen in T-bet$^{-/-}$ cultures (Fig 3A). This indicates that the requirement for STAT1 in promoting IL-12-dependent IFNγ production by WT cells (see Fig 1) is at least partially independent of STAT1-dependent T-bet induction.

The frequency of IFNγ^{+} cells within the STAT1$^{-/-}$ donor population in IAV-infected lungs was reduced about 30% versus that of T-bet$^{-/-}$ cells and was similar to that of T/S1$^{-/-}$ cells (Fig 3B). This is surprising given the detectable, albeit low, T-bet levels in at least some IAV-primed STAT1$^{-/-}$ cells seen in Figure 2. TNF production was also reduced in STAT1$^{-/-}$ and T/S1$^{-/-}$ versus in T-bet$^{-/-}$ cells (Fig 3C). In contrast, IL-2^{+} cells were increased in STAT1$^{-/-}$ versus T-bet$^{-/-}$ cells, and trended higher in T/S1$^{-/-}$ versus T-bet$^{-/-}$ cells (Fig 3D), consistent with a weaker Th1 functional imprint in cells lacking STAT1 expression.

Interestingly, Eomes was increased in STAT1$^{-/-}$ and in T/S1$^{-/-}$ versus in T-bet$^{-/-}$ cells (Fig 3E). These findings indicate that while Eomes induction in IAV-primed CD4 T cells does not require STAT1, optimal Th1 cytokine production by T-bet$^{-/-}$ cells, which we showed previously requires Eomes (14), is STAT1-dependent.

During IAV infection, autocrine IL-2 production induced by CD4 T cell effectors recognizing viral Ag upregulates their expression of CD127 (IL-7 receptor α chain) which in turn promotes memory fitness (31, 32). We also found that T-bet$^{-/-}$ effector cells produce more IL-2 and express higher levels of CD127 at 7 dpi with PR8-OVA$_{II}$ than do WT cells, which correlates with improved memory fitness of T-bet$^{-/-}$ versus WT effectors following the resolution of infection (13). However, despite being marked by stronger IL-2 production capacity versus T-bet$^{-/-}$ cells, both STAT1$^{-/-}$ and T/S1$^{-/-}$ cells expressed CD127 only at levels equivalent to WT cells at 7 dpi (Fig 3F). This suggests that at least some elements of improved memory fitness of T-bet$^{-/-}$ versus WT CD4 T cells primed by IAV may be STAT1-dependent.

IL-10 production during IAV infection is restricted largely to CD4 T cells in the lungs that co-produce high levels of IFNγ (33). As T-bet expression does not impact IL-10 production by IAV-primed CD4 T cells (13), we tested whether it is impacted by STAT1. Indeed, the frequency of IL-10^{+} cells was reduced about 80% in STAT1$^{-/-}$ and in T/S1$^{-/-}$ versus in T-bet$^{-/-}$ and in WT cells (Fig 3G), indicating that IL-10 production is STAT1-dependent but T-bet-independent in this setting.

IL-10 signals inhibit Th17 differentiation during IAV infection (33). Furthermore, IAV-primed T-bet$^{-/-}$ cells develop a cohort of Th17 effectors that is not seen during WT CD4 T cell responses (13), consistent with T-bet's restriction of Rorγt-dependent Th17 differentiation (34). Given the impaired expression of both IL-10 and T-bet by STAT1$^{-/-}$ versus WT cells, we hypothesized that STAT1$^{-/-}$ effectors would develop robust Th17 hallmarks. However, neither STAT1$^{-/-}$ nor T/S1$^{-/-}$ donor populations contained many Rorγt^{+} cells while about 40% of T-bet$^{-/-}$ cells in the same experiments were Rorγt^{+} (Fig 3H and I). In line with this pattern, few STAT1$^{-/-}$ or T/S1$^{-/-}$ cells produced IL-17 compared to about 15% of T-bet$^{-/-}$ cells were IL-17^{+} (Fig 3J). The STAT1$^{-/-}$ and T/S1$^{-/-}$ cells also did not produce IL-22 while T-bet$^{-/-}$ cells did (Fig 3J). These findings are unexpected as STAT1 activation is strongly associated with the suppression of Th17 development (35–37). Indeed, when plated in Th17-polarizing conditions *in vitro*, STAT1$^{-/-}$ and T/S1$^{-/-}$ cultures contained more IL-17^{+} cells than did T-bet$^{-/-}$ cultures (Supplemental Figure 4). Our results thus reveal a novel role for CD4 T cell-intrinsic STAT1 in promoting Th17 responses *in vivo* during viral infection.

Type I IFN restricts Th17 functionality in IAV-primed STAT1$^{-/-}$ CD4 T cells

The *in vitro* experiments presented in Supplemental Figure 4 suggested that STAT1 may not be required for pro-Th17 signaling during IAV infection, but instead could be required to prevent the integration of a signal able to suppress Th17 development. We reasoned that type I IFN could represent such a signal as it has been found to induce IFNγ production by STAT1$^{-/-}$ but not WT CD8 T cells through a STAT4-dependent mechanism (38, 39). In agreement with these studies, we observed strong STAT4 phosphorylation

when Ag-activated STAT1$^{-/-}$ OT-II cells were stimulated with type I IFN *in vitro* (Fig 4A). Furthermore, culturing WT, STAT1$^{-/-}$, or STAT4$^{-/-}$ OT-II cells in Th0 conditions supplemented with type I IFN promoted robust IFNγ production only from STAT1$^{-/-}$ cells (Fig 4B). This correlated with higher levels of T-bet and Eomes detected in STAT1$^{-/-}$ effectors compared to WT and STAT4$^{-/-}$ cells (Fig 4C and D). Thus, in the absence of CD4 T cell-intrinsic STAT1 expression, direct type I IFN signals can promote strong Th1-polarization *in vitro*.

Given the results presented above, we reasoned that type I IFN signals received by STAT1$^{-/-}$ cells responding to IAV may support their residual Th1 functionality and suppress Th17 development. To test this, we treated WT mice receiving STAT1$^{-/-}$ OT-II cells with blocking Ab against type I IFN receptor during PR8-OVA$_{II}$ infection. Treatment reduced IFNγ production by STAT1$^{-/-}$ cells (Fig 4E), correlating with decreases in T-bet and Eomes expression compared to cells in mice treated with isotype Ab (Fig 4F). In contrast, an 8-fold increase in Rorγt^{+} cells (Fig 4G) and roughly 6-fold increases in IL-17^{+} and IL-22^{+} cells (Fig 4H) were seen when type I IFN signaling was blocked. These levels of Rorγt and Th17 cytokine production are similar to those seen in T-bet$^{-/-}$ cells (see Fig 3). Importantly, Th1 cytokine production was similar in CD44^{high} WT host CD4 T cells in the lungs of mice treated with type I IFN receptor blocking or control Ab, with very few Th17 cytokine-producing cells seen regardless of treatment (Fig 4I). These results indicate a specific impact of type I IFN in promoting Th1 and repressing Th17 development by STAT1$^{-/-}$ CD4 T cells during IAV infection.

STAT4 is dispensable for IAV-primed Th1 identity in WT and T-bet$^{-/-}$ CD4 T cells

We next compared WT and STAT4$^{-/-}$ donor cells responding in separate IAV-primed WT mice. Numbers of WT and STAT4$^{-/-}$ cells in the infected lungs at 7 dpi were similar (Fig 5A), as was their expression of the T-bet-dependent surface markers CXCR3, Ly6C, and CD11a (not shown). T-bet itself was, however, slightly reduced in STAT4$^{-/-}$ cells (Fig 5B), while Eomes was not impacted (Fig 5C). Despite their marginally reduced expression of T-bet, production of IFNγ, TNF, and IL-2 by STAT4$^{-/-}$ and WT cells was comparable (Fig 5D), as was their expression of CD127 (Fig 5E). Finally, IL-10^{+} cells were similar between WT and STAT4$^{-/-}$ cells, with very few Rorγt^{+}, IL-17^{+} or IL-22^{+} cells detected in either population (not shown). Thus, in contrast to STAT1's critical regulatory roles, CD4 T cell-intrinsic STAT4 is not required to prime the phenotypic and functional Th1 hallmarks of WT effector cells responding to IAV.

We reasoned that the high levels of T-bet seen in WT and STAT4$^{-/-}$ CD4 T cells could negate requirements for the STAT4 pathway in regulating IAV-driven effector development, but that STAT4 could play a more prominent role in promoting Th1 functionality in T-bet$^{-/-}$ cells. To test the validity of this concept, we generated T-bet$^{-/-}$/STAT4$^{-/-}$ (T/S4$^{-/-}$) mice and first cultured naive T-bet$^{-/-}$ or T/S4$^{-/-}$ OT-II cells *in vitro* in Th1 conditions. IFNγ production was dramatically reduced in T/S4$^{-/-}$ versus T-bet$^{-/-}$ cultures (Fig 5F), confirming robust STAT4-dependent, T-bet-independent Th1 functionality. In contrast, numbers of T-bet$^{-/-}$ and T/S4$^{-/-}$ donor cells responding to IAV in WT mice (Fig 5G), as well as their production of IFNγ, TNF, IL-2 (Fig 5H), and IL-10 (Fig 5I), was similar.

We reasoned that STAT4 activation could antagonize IL-17 production by T-bet$^{-/-}$ cells, or alternatively, that it may be required for it given STAT4's role in Th17 priming under some conditions (18). However, T-bet$^{-/-}$ and T/S4$^{-/-}$ donors were marked by similar frequencies of IL-17^{+} (Fig 5J) and IL-22^{+} cells (not shown). Finally, in contrast to the impaired CD127 upregulation by T-bet$^{-/-}$ cells deficient for STAT1, levels of CD127 on T/S4$^{-/-}$ and T-bet$^{-/-}$ effector cells were similar (Fig 5K). Together these results indicate that the STAT4 pathway does not play a major role in promoting functional or phenotypic attributes of WT or T-bet$^{-/-}$ effectors primed by IAV.

STAT4 activation by IL-12 enhances the Th1 identity of IAV-primed CD4 T cells

The stark differences between the Th1 imprints of STAT4$^{-/-}$ and WT effectors primed *in vitro* under Th1 conditions seen in Figure 1 versus their similarity during IAV infection seen in Figure 5 suggests that WT cells may not be able to engage STAT4 in the latter setting. To test this, we treated mice receiving WT or STAT4$^{-/-}$ OT-II cells with IL-12 or with PBS alone by i.p. injection from 2–6 dpi and analyzed the donor cells at 7 dpi. We first assessed expression of a subunit of the IL-18 receptor (CD218a) known to be upregulated in a STAT4-dependent manner (40). The MFI of CD218a was increased about 3-fold on WT but not STAT4$^{-/-}$ donor cells by IL-12 treatment (Fig 6A), validating robust STAT4 engagement. T-bet expression by WT, but not STAT4$^{-/-}$ cells, was also markedly increased by IL-12 treatment (Fig 6B). Surprisingly, although most WT CD4 T cells in the lung are T-bet^{+} (6), using donor cells from the IL-12-treated mice to set a gate revealed only about about 20% of WT cells to be T-bet^{high} in control mice. The expression of Eomes by WT but not STAT4$^{-/-}$ cells was also increased by IL-12 treatment (Fig 6C), consistent with our *in vitro* findings of synergy between STAT1 and STAT4 activation in promoting Eomes induction. Functionally, IL-12 treatment nearly doubled the frequency of IFNγ^{+} WT cells (Fig 6D) and increased the MFI of the IFNγ^{+} cells about 3-fold, indicating enhanced per-cell production (Fig 6E). Unexpectedly, IL-12 treatment also increased the frequency of IFNγ^{+} STAT4$^{-/-}$ donor cells, though to a lesser extent, but it did not impact the MFI of the IFNγ^{+} cells.

We next treated recipients of T-bet$^{-/-}$ or T/S4$^{-/-}$ cells with IL-12 to determine the extent to which the STAT4-dependent pro-Th1 impacts of IL-12 are due to increased T-bet expression as seen in Figure 6B. IL-12 treatment marginally increased IL-18 receptor expression on T-bet$^{-/-}$ but not on T/S4$^{-/-}$ cells (Fig 6F). Given the 3-fold increase in MFI of WT cells treated with IL-12 in Figure 5A, this indicates that T-bet is required for maximal STAT4-dependent upregulation of IL-18 receptor. In further contrast to WT cells, production of IFNγ by T-bet$^{-/-}$ and T/S4$^{-/-}$ cells was not increased by IL-12 treatment (Fig 6G). The MFI of the IFNγ^{+} T-bet$^{-/-}$ cells was, however, increased slightly while that of T/S4$^{-/-}$ IFNγ^{+} cells was decreased by IL-12 treatment (Fig 6H). These results indicate that the pro-Th1 impact of STAT4 activation in CD4 T cells by IL-12 is primarily T-bet-dependent.

Elevated systemic production of IFNγ and/or other pro-inflammatory impacts of *in vivo* IL-12 administration in mice seen using similar IL-12 treatment regimens (41) could be required in addition to CD4 T cell-intrinsic STAT4 activation for some or all of the elements of boosted Th1 identity seen above. To test this, we transferred WT OT-II cells

to mice deficient for IL-12 receptor β (IL-12Rβ$^{-/-}$), infected the mice with IAV, and treated them with IL-12 or PBS alone (Fig 6I). pSTAT4 analysis at 7 dpi revealed increased STAT4 phosphorylation in donor, but not host, T cells in mice treated with IL-12 (Fig 6J), as expected. Importantly, IL-12 treatment increased WT donor cell expression of IL-18 receptor (Fig 6K), T-bet (Fig 6L), Eomes (Fig 6M), as well as the frequency (Fig 6N) and MFI (Fig 6O) of IFNγ^{+} cells. Together, these results demonstrate that IAV induces a submaximal Th1 imprint that can be markedly enhanced by therapeutic CD4 T cell-intrinsic STAT4 activation.

Combined STAT1 and STAT4 activation improves Th1-primed CD4 T cell protection against IAV

The results above suggest that synergy between STAT1 and STAT4 activation in CD4 T cells to strengthen their Th1 imprint may improve their protective efficacy against IAV. To test this, we primed naive WT, STAT1$^{-/-}$, or STAT4$^{-/-}$ OT-II cells with APC and peptide in the presence of IFNγ and IL-12 as in Figure 1. We then gave 3×10^{6} of the resulting effectors to naive WT mice and challenged them with 2 LD_{50} PR8-OVA_{II}. This number of WT Th1 effectors transfers robust protection to unprimed mice against otherwise lethal doses of PR8-OVA_{II} (13). As STAT1$^{-/-}$ CD4 T cells are eliminated by NK cells in WT mice during IAV infection (see Figure 2), we depleted NK cells in all groups of mice prior to effector transfer to normalize host environments during IAV infection.

We first assessed the Th1 attributes of the effector cells in the lungs at 4 dpi, the peak of their response after transfer in this model (42). STAT1$^{-/-}$ cells expressed less Ly6C than WT or STAT4$^{-/-}$ effectors (Fig 7A), consistent with its regulation by STAT1 as seen in Figure 5, while STAT4$^{-/-}$ effectors expressed less IL-18 receptor than WT or STAT1$^{-/-}$ effectors, consistent with its regulation by STAT4 as seen in Figure 6 (Fig 7B). Furthermore, WT cells expressed more T-bet than either STAT$^{-/-}$ population, consistent with expression patterns prior to transfer as seen in Fig 1 (Fig 7C). WT effectors also produced more IFNγ (Fig 7D and E) and TNF (Fig 7F) than STAT1$^{-/-}$ and especially STAT4$^{-/-}$ cells. In contrast, the STAT1$^{-/-}$ and STAT4$^{-/-}$ cells produced more IL-2 (Fig 7G), consistent with a weaker functional Th1 imprint. Th17 cytokines were not detected from any population (not shown).

We next assessed the ability of the transferred effectors to protect the unprimed mice against IAV-induced disease by assessing weight loss kinetics as well as viral control at 7 dpi. WT effectors promoted recovery of weight loss compared to mice not receiving cells and mice receiving STAT4$^{-/-}$ effectors, both of which continued to lose weight through 7 dpi (Fig 7H). Recipients of STAT1$^{-/-}$ cells lost more weight than WT recipients but they did begin to recover, albeit 1 or 2 days later than WT recipients, resulting in significantly less weight recovery by STAT1$^{-/-}$ versus WT recipients at 7 dpi (Fig 7H). Furthermore, mice receiving WT but not STAT4$^{-/-}$ cells controlled viral copies by over one log versus mice not receiving effector cells (Fig 7I). Interestingly, despite differences in weight loss, viral control in STAT1$^{-/-}$ recipients was similar to that mediated by WT effectors (Fig 7I).

Finally, we asked the extent to which the antiviral impact of the Th1-primed STAT1$^{-/-}$ effector cells is dependent on T-bet. In experiments transferring Th1-primed WT or T/S1$^{-/-}$ effectors to WT hosts, weight loss kinetics (not shown) and pulmonary viral copies detected

at 7 dpi were similar in T/S1$^{-/-}$ recipients relative to mice not receiving cells while WT effectors again promoted robust protection highlighted by significant viral control (Fig 7J). STAT4 activation during priming in the absence of T-bet expression thus cannot promote effective antiviral CD4 T cell responses. Together, our findings indicate that protection provided by Th1 effectors against IAV is T-bet-dependent and maximal when both STAT1 and STAT4 are engaged during priming.

Discussion

The mechanisms governing canonical Th subset polarization have been primarily defined in controlled *in vitro* settings. Overlaying these rules onto responses against pathogens *in vivo* has revealed important caveats and novel modes of regulation impacting not only CD4 T cell function, but also their capacity to protect against disease. Here, we show that CD4 T cell-intrinsic STAT4 does not impact the phenotypic or functional Th1 attributes that mark WT cells primed by IAV, an infection often cited as an exemplar of inducing a strong Th1 response. In contrast, STAT1 is required to promote effectors expressing Th1 hallmarks at WT levels, and more importantly, to prevent the deletion of virus-activated CD4 T cells by NK cells. NK cell activity induced by IAV infection is greatest in the lungs (43, 44). This is in line with the near total ablation of STAT1$^{-/-}$ cells in the lungs of mice with an intact NK cell compartment, with more STAT1$^{-/-}$ cells found in dLN and spleen. The full set of signals sensitizing STAT1$^{-/-}$ CD4 T cells to NK cell killing is unclear, but important to elucidate given this mechanism's potential to impact disease outcomes (45). Decreased expression of MHC-I and Qa-2 have been correlated with predisposing CD4 T cells to NK cell attack in a non-infectious *in vivo* model (28) and we found expression of both to be reduced on STAT1$^{-/-}$ versus WT cells responding to IAV. We also speculate that increased IL-2 production by STAT1$^{-/-}$ versus WT CD4 T cells may contribute to their enhanced susceptibility to NK cell killing by promoting local NK cell activation (29). Defining the mechanisms by which NK cells eliminate the STAT1$^{-/-}$ effectors in our study also requires further investigation. However, we previously showed that several NK cell receptors redundantly, and to some extent collaboratively, promote CD4 T cell killing in co-cultures of *in vitro*-generated WT Th-polarized effectors and NK cells from LCMV-infected mice (46). We also note that as we observed robust endogenous antiviral CD4 T cell responses in STAT1$^{-/-}$ mice, STAT1 activation in NK cells appears to be critical in promoting their ability to kill IAV-primed CD4 T cells.

We found that the production of Th1-associated cytokines is compromised more severely in STAT1$^{-/-}$ than in T-bet$^{-/-}$ cells responding to IAV. Our *in vivo* and *in vitro* data indicates that some elements of STAT1-dependent control of effector function are thus independent from its role in promoting T-bet induction. A clear example of this is that IL-10 production, which is largely restricted to IFNγ^{+} cells during IAV infection (33), is STAT1- but not T-bet-dependent. Nevertheless, about 25% of IAV-primed T/S1$^{-/-}$ effector cells are still capable of IFNγ production. We showed recently that IFNγ production by T-bet$^{-/-}$ CD4 T cells is Eomes-dependent (14). In vitro, Eomes expression is maximal in Th1-primed cells and significantly reduced in cells primed with IFNγ or IL-12 alone, indicating synergy between STAT1 and STAT4 in inducing its expression. IL-12 treatment of IAV-infected mice also boosted Eomes expression by CD4 T cells in a STAT4-dependent manner, consistent

with this pattern. However, IAV-primed STAT1$^{-/-}$ and T/S1$^{-/-}$ cells both expressed more Eomes than did T-bet$^{-/-}$ cells, which are themselves marked by higher levels of Eomes compared to WT cells. Indeed, regulation of Eomes by several mechanisms outside of the STAT1-STAT4-T-bet axis have been described (15), and our findings here suggest that such pathways may gain prominence when T-bet expression in CD4 T cell effectors is low or absent. We tried to generate STAT1$^{-/-}$/STAT4$^{-/-}$ double knockout mice to further investigate this possibility but were unsuccessful. This may be due to the tight linkage of STAT1 and STAT4 on mouse chromosome 1 (47). An alternative means of eliminating STAT1 and STAT4 expression within the same CD4 T cell, perhaps through CRISPR or a similar approach, is thus required.

Higher CD127 expression on T-bet$^{-/-}$ cells correlates with their ability to outcompete WT cells with the same TcR specificity to form memory following IAV clearance (13). Our data here suggests that STAT1 engagement may promote memory fitness in T-bet$^{-/-}$ effectors as STAT1$^{-/-}$ and T/S1$^{-/-}$ effectors expressed less CD127 than T-bet$^{-/-}$ cells. However, we found that other markers implicated in memory fate, such as Ly6C (48), and TCF1 (49) (not shown) were not impacted by STAT1-deficincy in T-bet$^{-/-}$ cells. Further experiments are thus required to determine the extent to which circulating and lung-resident memory generation, which can be maintained in the absence of IL-7 (50), is impacted by the STAT1 pathway in CD4 T cells during IAV infection.

STAT1 activation is linked with the suppression of Th17 development in mice and humans in a variety of settings (51–56). A major mechanism by which STAT1 acts in this regard is by promoting the expression of T-bet in response to STAT1-dependent pro-Th1 cytokines like IFNγ. Indeed, WT cells primed by IAV, that express relatively high levels of T-bet, do not develop a strong Th17 component while a sizeable Th17 cohort does develop in T-bet$^{-/-}$ CD4 T cells in response to IL-6 and TGFβ signals in the infected lung (13, 14). It is thus surprising that we found a requirement for STAT1 expression by IAV-primed T-bet$^{-/-}$ CD4 T cells to promote Rorγt and hallmark Th17 functionality. However, blocking type I IFN signaling in IAV-infected mice restored Th17 responses by STAT1$^{-/-}$ cells that were similar in magnitude to those of T-bet$^{-/-}$ cells. Based on previous studies with CD8 T cells (38, 39) and the *in vitro* data presented here, type I IFN appears to act as a pro-Th1 factor during IAV infection in the absence of CD4 T cell-intrinsic STAT1 by signaling through STAT4. This in turn promotes expression of T-bet, Eomes, and IFNγ, and the concomitant repression of Th17 programming. This mechanism at first glance seems incompatible with the easily detectable Th17 cells in full STAT1$^{-/-}$ mice infected with IAV (25). However, the IAV-induced inflammatory environment in STAT1$^{-/-}$ mice is likely sufficiently altered from that in WT mice to nullify the requirement for STAT1 expression to enable Th17-polarization. This position is supported by our finding that even WT OT-II cells produce IL-17 in IAV-infected STAT1$^{-/-}$, but not STAT4$^{-/-}$ or WT hosts. That viral control in WT and STAT1$^{-/-}$ mice was similar in these experiments is also perhaps unexpected given STAT1's key role in type I and type III signaling, and the antiviral impacts of these pathways reported in many murine IAV studies (57). However, similar IAV titers in WT and STAT1$^{-/-}$ mice have been reported previously (25, 58), suggesting that type I and/or III IFNs may signal through a non-canonical STAT1-independent pathway (59) in the STAT1$^{-/-}$ mice to promote efficient IAV control. In contrast to the critical role for STAT1 expression

by CD4 T cells in promoting Th17 responses, STAT4 did not impact Th17 functionality in T-bet$^{-/-}$ CD4 T cells responding to IAV despite its association with Th17 development in some studies. This fits our findings that Th17 development during IAV infection requires IL-6 and TGF-β (14), and that STAT4 seems to promote IL-23-dependent, but not IL-6/TGF-β-dependent Th17 programing (60).

The broad similarities between WT and STAT4$^{-/-}$ CD4 T cell responses against IAV are surprising as in contrast to some viruses like LCMV that do not induce robust IL-12 (61), IAV induces IL-12 at levels that are sufficient to impact elements of innate immune defense (62, 63). We postulate that IAV-induced IL-12 may be segregated physically or temporally from microenvironments where virus-specific CD4 T cells are primed. Indeed, macrophages appear to be a major producer of IL-12 during IAV infection (64) while its production is not detected from IAV-infected dendritic cells (65), which are the major APC involved in T cell priming. However, by treating IAV-primed mice with exogenous IL-12, we show that multiple aspects of Th1 identity can be enhanced through CD4 T cell-intrinsic STAT4 activation, and that this boost is ultimately T-bet-dependent. We speculate that the 'weak' Th1 imprint induced in WT cells may underlie at least some aspects of the remarkable heterogeneity seen within the bulk IAV-primed CD4 T cell effector populations during both primary and recall responses (11, 66).

Our findings of improved protection mediated by effector cells with stronger versus weaker Th1 identify generated by engaging both STAT1 and STAT4 during priming agree with patterns found analyzing memory CD4 T cell-mediated protection against IAV. For example, we found previously that the transfer of Th1-polarized memory cells protected naive mice from lethal infection while Th0 memory cells, that adopt weaker Th1 attributes *in vivo*, were less effective (67). Similarly, Farber and colleagues found that while the transfer of lung-retentive memory cells from IAV-primed mice protected naive mice against a lethal IAV challenge, an equal number of memory cells isolated from the spleen could not (68). The lung-derived cells in this study were marked by enhanced IFNγ and reduced IL-2 production versus the splenic cells (68), matching the cytokine production patterns correlating with maximal protection provided by WT versus STAT1$^{-/-}$ and especially STAT4$^{-/-}$ effector cells primed in Th1 conditions. This supports the concept that vaccine strategies incorporating IL-12, or IL-12-inducing adjuvants, to boost Th1 polarization may improve CD4 T cell immunity, and that this pathway supporting Th1 induction is not redundant to that initiated by STAT1 activation. Further studies are required to determine those STAT4-dependent genes induced by IL-12 that promote improved protective capacity. One potential mechanism is the IL-12-mediated upregulation of IL-18 receptor, as IL-18 has been shown to enhance cytokine production by mucosal associated invariant T cells (69) and CD8 T cells responding to IAV (70). Vaccines targeting STAT4 activation in CD4 T cells may be particularly relevant to neonates and the aged that are marked by increased susceptibility to IAV and by weaker T cell responses. Indeed, murine studies suggest that IL-12 signals can improve vaccine efficacy in these groups, though the underlying mechanisms have not been defined (71, 72).

In summary, we show that CD4 T cell-intrinsic STAT1 is needed for the Th1 hallmarks expressed by WT CD4 T cells primed by IAV, and to prevent their deletion by NK cells.

Unexpectedly, STAT1 is also required to promote Th17 responses against IAV that develop in the absence of CD4 T cell-intrinsic T-bet expression, and that are highly protective in their own right (14, 33). In contrast, although it is crucial in directing canonical Th1-polarization *in vitro*, we find that the STAT4 pathway plays a minimal role in promoting antiviral CD4 T cell responses. Our findings are consistent with recent work indicating that the STAT4-dependent activation module is more prominently engaged during phagosomal versus viral infections (73). However, we show that STAT4 activation in IAV-primed CD4 T cells maximizes their Th1 imprint and promotes a robust T-bet-dependent antiviral effector program that STAT1 activation in the absence of STAT4 engagement cannot. This indicates that STAT1 and STAT4 are non-redundant in terms of promoting effective 'Th1' cells in the setting of IAV infection. Our findings thus stress that care should be taken when characterizing responses as 'Th1' based on the presence of Th1 attributes and relative absence of those defining other subsets. Instead, they highlight important gradations in Th1 identity that can help to predict the ability of CD4 T cells to combat viruses, and that can be modulated to improve outcomes.

Supplementary Material

Refer to Web version on PubMed Central for supplementary material.

Acknowledgements

We thank the University of Central Florida Lake Nona Vivarium staff for excellent care of the mice used in these studies and the UCF flow cytometry core facility. The graphical abstract was created with BioRender.com.

This work was supported by NIH grant R21 AI146647 and R01 AI167994 (to K.K.M.), funds provided by the University of Central Florida (K.K.M. and T.M.S.), by a University of Central Florida Doctoral Support Award (C.M.F.) and by a Solomon Klotz Excellence in Immunology and Allergy Award (C.M.F.). The funders had no role in the design or conduct of the study, nor in the collection, analysis, or interpretation of data. The funders had no role in the preparation, review, or approval of the manuscript.

References

1. Swain SL, McKinstry KK, and Strutt TM. 2012. Expanding roles for CD4(+) T cells in immunity to viruses. Nat Rev Immunol 12: 136–148. [PubMed: 22266691]
2. Sant AJ, Richards KA, and Nayak J. 2018. Distinct and complementary roles of CD4 T cells in protective immunity to influenza virus. Curr Opin Immunol 53: 13–21. [PubMed: 29621639]
3. Belz GT, Wodarz D, Diaz G, Nowak MA, and Doherty PC. 2002. Compromised influenza virus-specific CD8(+)-T-cell memory in CD4(+)-T-cell-deficient mice. J Virol 76: 12388–12393. [PubMed: 12414983]
4. Eichelberger M, Allan W, Zijlstra M, Jaenisch R, and Doherty PC. 1991. Clearance of influenza virus respiratory infection in mice lacking class I major histocompatibility complex-restricted CD8+ T cells. J Exp Med 174: 875–880. [PubMed: 1919440]
5. Brown DM, Lee S, Garcia-Hernandez Mde L, and Swain SL. 2012. Multifunctional CD4 cells expressing gamma interferon and perforin mediate protection against lethal influenza virus infection. J Virol 86: 6792–6803. [PubMed: 22491469]
6. Strutt TM, McKinstry KK, Kuang Y, Bradley LM, and Swain SL. 2012. Memory CD4+ T-cell-mediated protection depends on secondary effectors that are distinct from and superior to primary effectors. Proc Natl Acad Sci U S A 109: E2551–2560. [PubMed: 22927425]
7. Jansen JM, Gerlach T, Elbahesh H, Rimmelzwaan GF, and Saletti G. 2019. Influenza virus-specific CD4+ and CD8+ T cell-mediated immunity induced by infection and vaccination. J Clin Virol 119: 44–52. [PubMed: 31491709]

8. McKinstry KK, Dutton RW, Swain SL, and Strutt TM. 2013. Memory CD4 T cell-mediated immunity against influenza A virus: more than a little helpful. Arch Immunol Ther Exp (Warsz) 61: 341–353. [PubMed: 23708562]

9. Wilkinson TM, Li CK, Chui CS, Huang AK, Perkins M, Liebner JC, Lambkin-Williams R, Gilbert A, Oxford J, Nicholas B, Staples KJ, Dong T, Douek DC, McMichael AJ, and Xu XN. 2012. Preexisting influenza-specific CD4+ T cells correlate with disease protection against influenza challenge in humans. Nat Med 18: 274–280. [PubMed: 22286307]

10. Ruterbusch M, Pruner KB, Shehata L, and Pepper M. 2020. In Vivo CD4(+) T Cell Differentiation and Function: Revisiting the Th1/Th2 Paradigm. Annu Rev Immunol 38: 705–725. [PubMed: 32340571]

11. Strutt TM, McKinstry KK, Marshall NB, Vong AM, Dutton RW, and Swain SL. 2013. Multipronged CD4(+) T-cell effector and memory responses cooperate to provide potent immunity against respiratory virus. Immunol Rev 255: 149–164. [PubMed: 23947353]

12. Swain SL, Agrewala JN, Brown DM, Jelley-Gibbs DM, Golech S, Huston G, Jones SC, Kamperschroer C, Lee WH, McKinstry KK, Roman E, Strutt T, and Weng NP. 2006. CD4+ T-cell memory: generation and multi-faceted roles for CD4+ T cells in protective immunity to influenza. Immunol Rev 211: 8–22. [PubMed: 16824113]

13. Dhume K, Finn CM, Strutt TM, Sell S, and McKinstry KK. 2019. T-bet optimizes CD4 T-cell responses against influenza through CXCR3-dependent lung trafficking but not functional programming. Mucosal Immunol 12: 1220–1230. [PubMed: 31278374]

14. Dhume K, Finn CM, Devarajan P, Singh A, Tejero JD, Prokop E, Strutt TM, Sell S, Swain SL, and McKinstry KK. 2022. Bona Fide Th17 Cells without Th1 Functional Plasticity Protect against Influenza. J Immunol 208: 1998–2007. [PubMed: 35338093]

15. Dhume K, Kaye B, and McKinstry KK. 2022. Regulation of CD4 T Cell Responses by the Transcription Factor Eomesodermin. Biomolecules 12.

16. Pritchard GH, Kedl RM, and Hunter CA. 2019. The evolving role of T-bet in resistance to infection. Nat Rev Immunol 19: 398–410. [PubMed: 30846856]

17. Zhu J, Jankovic D, Oler AJ, Wei G, Sharma S, Hu G, Guo L, Yagi R, Yamane H, Punkosdy G, Feigenbaum L, Zhao K, and Paul WE. 2012. The transcription factor T-bet is induced by multiple pathways and prevents an endogenous Th2 cell program during Th1 cell responses. Immunity 37: 660–673. [PubMed: 23041064]

18. Furuta S, Kagami S, Tamachi T, Ikeda K, Fujiwara M, Suto A, Hirose K, Watanabe N, Saito Y, Iwamoto I, and Nakajima H. 2008. Overlapping and distinct roles of STAT4 and T-bet in the regulation of T cell differentiation and allergic airway inflammation. J Immunol 180: 6656–6662. [PubMed: 18453585]

19. Thieu VT, Yu Q, Chang HC, Yeh N, Nguyen ET, Sehra S, and Kaplan MH. 2008. Signal transducer and activator of transcription 4 is required for the transcription factor T-bet to promote T helper 1 cell-fate determination. Immunity 29: 679–690. [PubMed: 18993086]

20. Usui T, Nishikomori R, Kitani A, and Strober W. 2003. GATA-3 suppresses Th1 development by downregulation of Stat4 and not through effects on IL-12Rbeta2 chain or T-bet. Immunity 18: 415–428. [PubMed: 12648458]

21. McKinstry KK, Golech S, Lee WH, Huston G, Weng NP, and Swain SL. 2007. Rapid default transition of CD4 T cell effectors to functional memory cells. J Exp Med 204: 2199–2211. [PubMed: 17724126]

22. Strutt TM, McKinstry KK, Dibble JP, Winchell C, Kuang Y, Curtis JD, Huston G, Dutton RW, and Swain SL. 2010. Memory CD4+ T cells induce innate responses independently of pathogen. Nat Med 16: 558–564, 551p following 564. [PubMed: 20436484]

23. Berenson LS, Farrar JD, Murphy TL, and Murphy KM. 2004. Frontline: absence of functional STAT4 activation despite detectable tyrosine phosphorylation induced by murine IFN-alpha. Eur J Immunol 34: 2365–2374. [PubMed: 15307169]

24. Hwang ES, Hong JH, and Glimcher LH. 2005. IL-2 production in developing Th1 cells is regulated by heterodimerization of RelA and T-bet and requires T-bet serine residue 508. J Exp Med 202: 1289–1300. [PubMed: 16275766]

25. Lee B, Gopal R, Manni ML, McHugh KJ, Mandalapu S, Robinson KM, and Alcorn JF. 2017. STAT1 Is Required for Suppression of Type 17 Immunity during Influenza and Bacterial Superinfection. Immunohorizons 1: 81–91. [PubMed: 29577113]
26. Bot A, Rodrigo E, Wolfe T, Bot S, and Von Herrath MG. 2003. Infection-triggered regulatory mechanisms override the role of STAT 4 in control of the immune response to influenza virus antigens. J Virol 77: 5794–5800. [PubMed: 12719572]
27. Thomas PG, Brown SA, Yue W, So J, Webby RJ, and Doherty PC. 2006. An unexpected antibody response to an engineered influenza virus modifies CD8+ T cell responses. Proc Natl Acad Sci U S A 103: 2764–2769. [PubMed: 16473934]
28. Kang YH, Biswas A, Field M, and Snapper SB. 2019. STAT1 signaling shields T cells from NK cell-mediated cytotoxicity. Nat Commun 10: 912. [PubMed: 30796216]
29. Arbelaez CA, Palle P, Charaix J, and Bettelli E. 2022. STAT1 signaling protects self-reactive T cells from control by innate cells during neuroinflammation. JCI Insight.
30. McKinstry KK, Alam F, Flores-Malavet V, Nagy MZ, Sell S, Cooper AM, Swain SL, and Strutt TM. 2019. Memory CD4 T cell-derived IL-2 synergizes with viral infection to exacerbate lung inflammation. PLoS Pathog 15: e1007989. [PubMed: 31412088]
31. McKinstry KK, Strutt TM, Bautista B, Zhang W, Kuang Y, Cooper AM, and Swain SL. 2014. Effector CD4 T-cell transition to memory requires late cognate interactions that induce autocrine IL-2. Nat Commun 5: 5377. [PubMed: 25369785]
32. Swain SL, Jones MC, Devarajan P, Xia J, Dutton RW, Strutt TM, and McKinstry KK. 2021. Durable CD4 T-Cell Memory Generation Depends on Persistence of High Levels of Infection at an Effector Checkpoint that Determines Multiple Fates. Cold Spring Harb Perspect Biol.
33. McKinstry KK, Strutt TM, Buck A, Curtis JD, Dibble JP, Huston G, Tighe M, Hamada H, Sell S, Dutton RW, and Swain SL. 2009. IL-10 deficiency unleashes an influenza-specific Th17 response and enhances survival against high-dose challenge. J Immunol 182: 7353–7363. [PubMed: 19494257]
34. Lazarevic V, Chen X, Shim JH, Hwang ES, Jang E, Bolm AN, Oukka M, Kuchroo VK, and Glimcher LH. 2011. T-bet represses T(H)17 differentiation by preventing Runx1-mediated activation of the gene encoding RORgammat. Nat Immunol 12: 96–104. [PubMed: 21151104]
35. Peters A, Fowler KD, Chalmin F, Merkler D, Kuchroo VK, and Pot C. 2015. IL-27 Induces Th17 Differentiation in the Absence of STAT1 Signaling. J Immunol 195: 4144–4153. [PubMed: 26408664]
36. Meyer Zu Horste G, Przybylski D, Schramm MA, Wang C, Schnell A, Lee Y, Sobel R, Regev A, and Kuchroo VK. 2018. Fas Promotes T Helper 17 Cell Differentiation and Inhibits T Helper 1 Cell Development by Binding and Sequestering Transcription Factor STAT1. Immunity 48: 556–569 e557. [PubMed: 29562202]
37. Villarino AV, Gallo E, and Abbas AK. 2010. STAT1-activating cytokines limit Th17 responses through both T-bet-dependent and -independent mechanisms. J Immunol 185: 6461–6471. [PubMed: 20974984]
38. Nguyen KB, Watford WT, Salomon R, Hofmann SR, Pien GC, Morinobu A, Gadina M, O'Shea JJ, and Biron CA. 2002. Critical role for STAT4 activation by type 1 interferons in the interferon-gamma response to viral infection. Science 297: 2063–2066. [PubMed: 12242445]
39. Gil MP, Ploquin MJ, Watford WT, Lee SH, Kim K, Wang X, Kanno Y, O'Shea JJ, and Biron CA. 2012. Regulating type 1 IFN effects in CD8 T cells during viral infections: changing STAT4 and STAT1 expression for function. Blood 120: 3718–3728. [PubMed: 22968462]
40. Nakahira M, Tomura M, Iwasaki M, Ahn HJ, Bian Y, Hamaoka T, Ohta T, Kurimoto M, and Fujiwara H. 2001. An absolute requirement for STAT4 and a role for IFN-gamma as an amplifying factor in IL-12 induction of the functional IL-18 receptor complex. J Immunol 167: 1306–1312. [PubMed: 11466347]
41. Morris SC, Madden KB, Adamovicz JJ, Gause WC, Hubbard BR, Gately MK, and Finkelman FD. 1994. Effects of IL-12 on in vivo cytokine gene expression and Ig isotype selection. J Immunol 152: 1047–1056. [PubMed: 7905496]

42. Brown DM, Dilzer AM, Meents DL, and Swain SL. 2006. CD4 T cell-mediated protection from lethal influenza: perforin and antibody-mediated mechanisms give a one-two punch. J Immunol 177: 2888–2898. [PubMed: 16920924]
43. Carlin LE, Hemann EA, Zacharias ZR, Heusel JW, and Legge KL. 2018. Natural Killer Cell Recruitment to the Lung During Influenza A Virus Infection Is Dependent on CXCR3, CCR5, and Virus Exposure Dose. Front Immunol 9: 781. [PubMed: 29719539]
44. Stegemann-Koniszewski S, Behrens S, Boehme JD, Hochnadel I, Riese P, Guzman CA, Kroger A, Schreiber J, Gunzer M, and Bruder D. 2018. Respiratory Influenza A Virus Infection Triggers Local and Systemic Natural Killer Cell Activation via Toll-Like Receptor 7. Front Immunol 9: 245. [PubMed: 29497422]
45. Waggoner SN, Cornberg M, Selin LK, and Welsh RM. 2012. Natural killer cells act as rheostats modulating antiviral T cells. Nature 481: 394–398.
46. Daniels KA, O'Donnell CL, Castonguay C, Strutt TM, McKinstry KK, Swain SL, and Welsh RM. 2020. Virus-induced natural killer cell lysis of T cell subsets. Virology 539: 26–37. [PubMed: 31670188]
47. Copeland NG, Gilbert DJ, Schindler C, Zhong Z, Wen Z, Darnell JE Jr., Mui AL, Miyajima A, Quelle FW, Ihle JN, and et al. 1995. Distribution of the mammalian Stat gene family in mouse chromosomes. Genomics 29: 225–228. [PubMed: 8530075]
48. Marshall HD, Chandele A, Jung YW, Meng H, Poholek AC, Parish IA, Rutishauser R, Cui W, Kleinstein SH, Craft J, and Kaech SM. 2011. Differential expression of Ly6C and T-bet distinguish effector and memory Th1 CD4(+) cell properties during viral infection. Immunity 35: 633–646. [PubMed: 22018471]
49. Nish SA, Zens KD, Kratchmarov R, Lin WW, Adams WC, Chen YH, Yen B, Rothman NJ, Bhandoola A, Xue HH, Farber DL, and Reiner SL. 2017. CD4+ T cell effector commitment coupled to self-renewal by asymmetric cell divisions. J Exp Med 214: 39–47. [PubMed: 27923906]
50. Strutt TM, Dhume K, Finn CM, Hwang JH, Castonguay C, Swain SL, and McKinstry KK. 2018. IL-15 supports the generation of protective lung-resident memory CD4 T cells. Mucosal Immunol 11: 668–680. [PubMed: 29186108]
51. Liu L, Okada S, Kong XF, Kreins AY, Cypowyj S, Abhyankar A, Toubiana J, Itan Y, Audry M, Nitschke P, Masson C, Toth B, Flatot J, Migaud M, Chrabieh M, Kochetkov T, Bolze A, Borghesi A, Toulon A, Hiller J, Eyerich S, Eyerich K, Gulacsy V, Chernyshova L, Chernyshov V, Bondarenko A, Grimaldo RM, Blancas-Galicia L, Beas IM, Roesler J, Magdorf K, Engelhard D, Thumerelle C, Burgel PR, Hoernes M, Drexel B, Seger R, Kusuma T, Jansson AF, Sawalle-Belohradsky J, Belohradsky B, Jouanguy E, Bustamante J, Bue M, Karin N, Wildbaum G, Bodemer C, Lortholary O, Fischer A, Blanche S, Al-Muhsen S, Reichenbach J, Kobayashi M, Rosales FE, Lozano CT, Kilic SS, Oleastro M, Etzioni A, Traidl-Hoffmann C, Renner ED, Abel L, Picard C, Marodi L, Boisson-Dupuis S, Puel A, and Casanova JL. 2011. Gain-of-function human STAT1 mutations impair IL-17 immunity and underlie chronic mucocutaneous candidiasis. J Exp Med 208: 1635–1648. [PubMed: 21727188]
52. Puel A 2020. Human inborn errors of immunity underlying superficial or invasive candidiasis. Hum Genet 139: 1011–1022. [PubMed: 32124012]
53. Feng G, Gao W, Strom TB, Oukka M, Francis RS, Wood KJ, and Bushell A. 2008. Exogenous IFN-gamma ex vivo shapes the alloreactive T-cell repertoire by inhibition of Th17 responses and generation of functional Foxp3+ regulatory T cells. Eur J Immunol 38: 2512–2527. [PubMed: 18792404]
54. Kulkarni MM, Varikuti S, Terrazas C, Kimble JL, Satoskar AR, and McGwire BS. 2015. Signal transducer and activator of transcription 1 (STAT-1) plays a critical role in control of Trypanosoma cruzi infection. Immunology 145: 225–231. [PubMed: 25545325]
55. Leon-Cabrera S, Vazquez-Sandoval A, Molina-Guzman E, Delgado-Ramirez Y, Delgado-Buenrostro NL, Callejas BE, Chirino YI, Perez-Plasencia C, Rodriguez-Sosa M, Olguin JE, Salinas C, Satoskar AR, and Terrazas LI. 2018. Deficiency in STAT1 Signaling Predisposes Gut Inflammation and Prompts Colorectal Cancer Development. Cancers (Basel) 10.

56. Marie IJ, Brambilla L, Azzouz D, Chen Z, Baracho GV, Arnett A, Li HS, Liu W, Cimmino L, Chattopadhyay P, Silverman G, Watowich SS, Khor B, and Levy DE. 2021. Tonic interferon restricts pathogenic IL-17-driven inflammatory disease via balancing the microbiome. Elife 10.
57. Wu W, and Metcalf JP. 2020. The Role of Type I IFNs in Influenza: Antiviral Superheroes or Immunopathogenic Villains? J Innate Immun 12: 437–447. [PubMed: 32564033]
58. Garcia-Sastre A, Durbin RK, Zheng H, Palese P, Gertner R, Levy DE, and Durbin JE. 1998. The role of interferon in influenza virus tissue tropism. J Virol 72: 8550–8558. [PubMed: 9765393]
59. Stanifer ML, Pervolaraki K, and Boulant S. 2019. Differential Regulation of Type I and Type III Interferon Signaling. Int J Mol Sci 20.
60. Mathur AN, Chang HC, Zisoulis DG, Stritesky GL, Yu Q, O'Malley JT, Kapur R, Levy DE, Kansas GS, and Kaplan MH. 2007. Stat3 and Stat4 direct development of IL-17-secreting Th cells. J Immunol 178: 4901–4907. [PubMed: 17404271]
61. Dalod M, Salazar-Mather TP, Malmgaard L, Lewis C, Asselin-Paturel C, Briere F, Trinchieri G, and Biron CA. 2002. Interferon alpha/beta and interleukin 12 responses to viral infections: pathways regulating dendritic cell cytokine expression in vivo. J Exp Med 195: 517–528. [PubMed: 11854364]
62. Monteiro JM, Harvey C, and Trinchieri G. 1998. Role of interleukin-12 in primary influenza virus infection. J Virol 72: 4825–4831. [PubMed: 9573248]
63. Hwang I, Scott JM, Kakarla T, Duriancik DM, Choi S, Cho C, Lee T, Park H, French AR, Beli E, Gardner E, and Kim S. 2012. Activation mechanisms of natural killer cells during influenza virus infection. PLoS One 7: e51858. [PubMed: 23300570]
64. Hama Y, Kurokawa M, Imakita M, Yoshida Y, Shimizu T, Watanabe W, and Shiraki K. 2009. Interleukin 12 is a primary cytokine responding to influenza virus infection in the respiratory tract of mice. Acta Virol 53: 233–240. [PubMed: 19941386]
65. Bhardwaj N, Seder RA, Reddy A, and Feldman MV. 1996. IL-12 in conjunction with dendritic cells enhances antiviral CD8+ CTL responses in vitro. J Clin Invest 98: 715–722. [PubMed: 8698863]
66. Strutt TM, McKinstry KK, and Swain SL. 2009. Functionally diverse subsets in CD4 T cell responses against influenza. J Clin Immunol 29: 145–150. [PubMed: 19050998]
67. McKinstry KK, Strutt TM, Kuang Y, Brown DM, Sell S, Dutton RW, and Swain SL. 2012. Memory CD4+ T cells protect against influenza through multiple synergizing mechanisms. J Clin Invest 122: 2847–2856. [PubMed: 22820287]
68. Teijaro JR, Turner D, Pham Q, Wherry EJ, Lefrancois L, and Farber DL. 2011. Cutting edge: Tissue-retentive lung memory CD4 T cells mediate optimal protection to respiratory virus infection. J Immunol 187: 5510–5514. [PubMed: 22058417]
69. Loh L, Wang Z, Sant S, Koutsakos M, Jegaskanda S, Corbett AJ, Liu L, Fairlie DP, Crowe J, Rossjohn J, Xu J, Doherty PC, McCluskey J, and Kedzierska K. 2016. Human mucosal-associated invariant T cells contribute to antiviral influenza immunity via IL-18-dependent activation. Proc Natl Acad Sci U S A 113: 10133–10138. [PubMed: 27543331]
70. Denton AE, Doherty PC, Turner SJ, and La Gruta NL. 2007. IL-18, but not IL-12, is required for optimal cytokine production by influenza virus-specific CD8+ T cells. Eur J Immunol 37: 368–375. [PubMed: 17219365]
71. Arulanandam BP, Mittler JN, Lee WT, O'Toole M, and Metzger DW. 2000. Neonatal administration of IL-12 enhances the protective efficacy of antiviral vaccines. J Immunol 164: 3698–3704. [PubMed: 10725728]
72. Khan T, Heffron CL, High KP, and Roberts PC. 2014. Tailored vaccines targeting the elderly using whole inactivated influenza vaccines bearing cytokine immunomodulators. J Interferon Cytokine Res 34: 129–139. [PubMed: 24102577]
73. Krueger PD, Goldberg MF, Hong SW, Osum KC, Langlois RA, Kotov DI, Dileepan T, and Jenkins MK. 2021. Two sequential activation modules control the differentiation of protective T helper-1 (Th1) cells. Immunity 54: 687–701 e684. [PubMed: 33773107]

Key Points

- STAT1 protects influenza-primed CD4 T cells from NK cell-mediated deletion
- STAT1 but not STAT4 is needed for Th1 and Th17 functionality in antiviral CD4 T cells
- Engaging STAT1 and STAT4 during priming maximizes protective CD4 T cell capacity

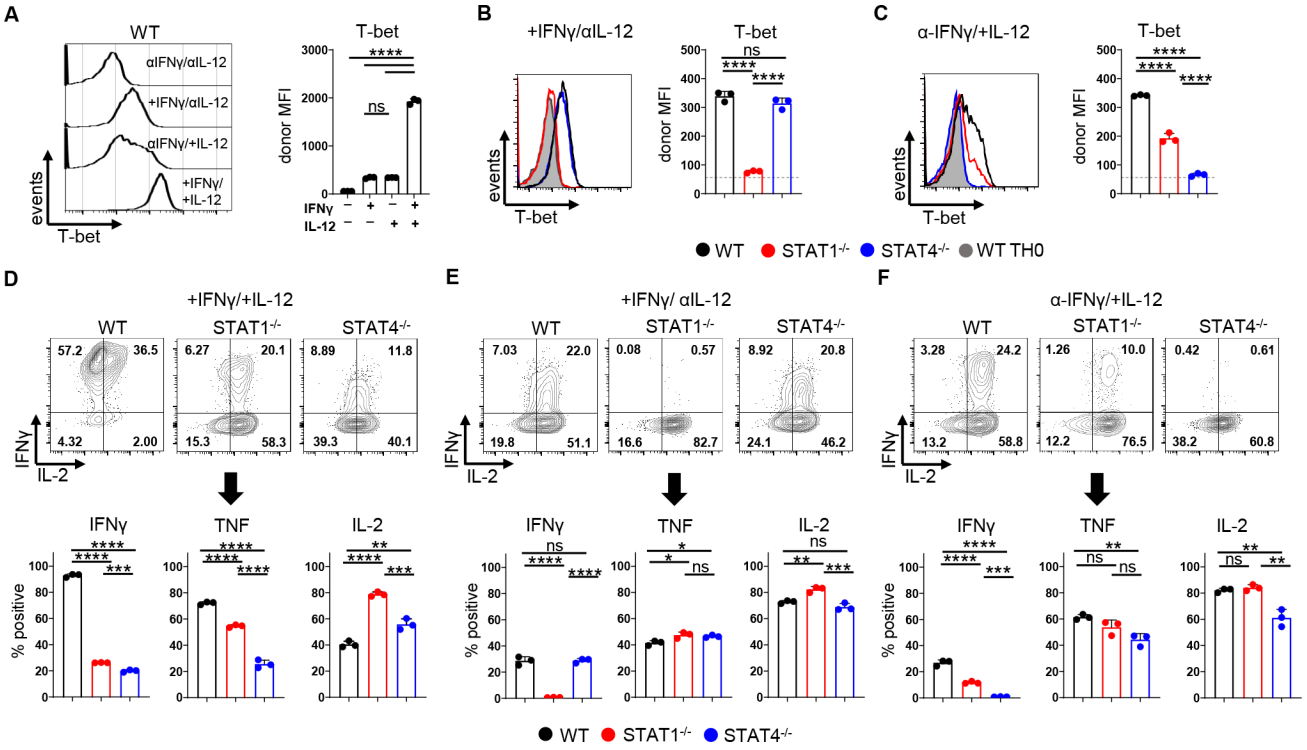

Figure 1: STAT1 and STAT4 activating cytokines synergize to promote Th1 differentiation in vitro.

Naive WT OT-II cells were cultured with APC and peptide and neutralizing Abs against IFNγ (αIFNγ) and IL-12 (αIL-12) (Th0 conditions), with IFNγ and αIL-12, with IL-12 and αIFNγ, or with IFNγ and IL-12 (Th1 conditions). **(A)** After 4 days, effector cells were analyzed for T-bet with representative staining (left) and the mean florescence intensity (MFI) from 3 wells per condition (right). WT, STAT1$^{-/-}$, or STAT4$^{-/-}$ OT-II cells were cultured with WT APC and peptide with **(B)** IFNγ and αIL-12 or **(C)** IL-12 and αIFNγ with T-bet expression including WT Th0 T-bet MFI as a filled grey histogram in representative plots and a dotted line in graphs. Representative staining of IFNγ and IL-2 production by WT, STAT1$^{-/-}$, and STAT4$^{-/-}$ OT-II cells (top) and summary analysis from 3 wells for IFNγ, TNF, and IL-2 production (beneath the arrows) in cultures supplemented with **(D)** IL-12 and IFNγ, **(E)** IFNγ and αIL-12, or **(F)** αIFNγ and IL-12. All results from 1 of 4 independent experiments.

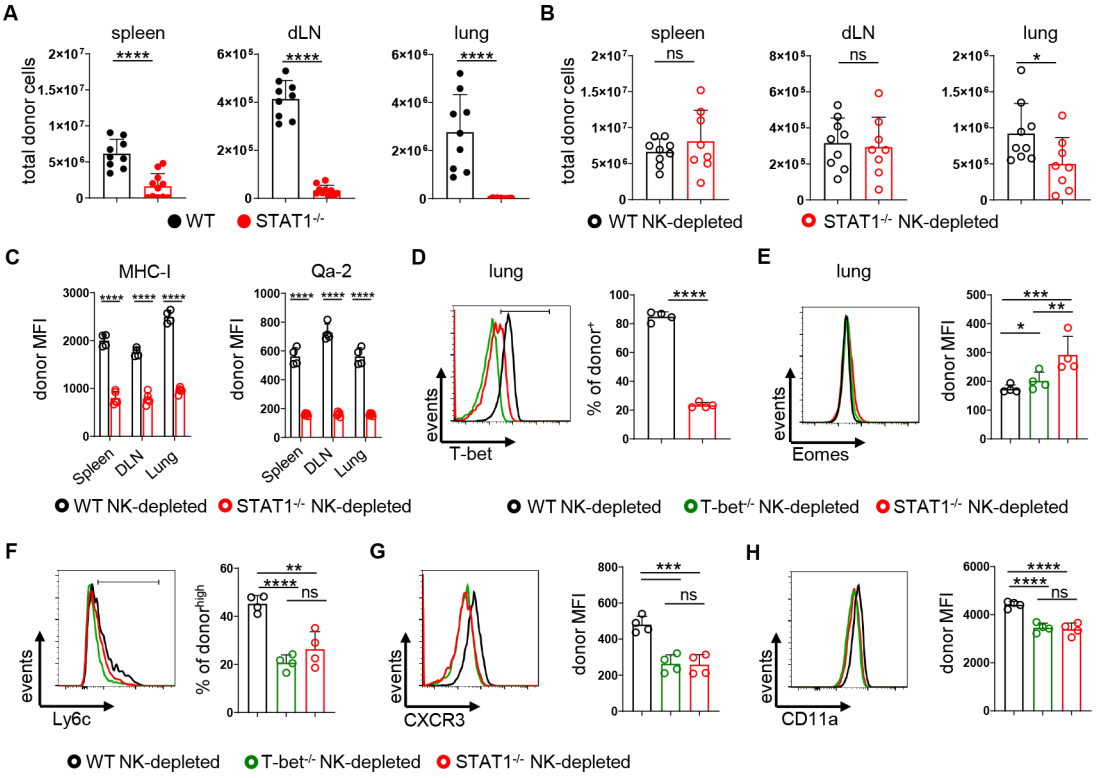

Figure 2: STAT1$^{-/-}$ CD4 T cells primed by IAV are susceptible to NK cell attack and lose Th1 identity.

1×10^6 naive WT or STAT1$^{-/-}$ OT-II cells were transferred to separate congenic WT hosts that were then primed with PR8-OVA$_{II}$. **(A)** Total donor cells in stated organs at 7 dpi. Results from individual mice pooled from 2 separate experiments. **(B)** Donor cell recovery at 7 dpi from congenic WT hosts that were depleted of NK cells prior to IAV infection. Results pooled from 2 individual experiments with **(C)** MHC-I and Qa-2 expression by WT and STAT1$^{-/-}$ donor cells responding in separate NK cell-depleted hosts. Results from 1 of 2 experiments. Representative staining of WT, T-bet$^{-/-}$, and STAT1$^{-/-}$ donor cells responding in the lungs of NK cell-depleted hosts at 7 dpi with summary analysis from 4 mice per group for **(D)** T-bet, **(E)** Eomes, **(F)** Ly6C, **(G)** CXCR3, and **(H)** CD11a. Data for D-G from one of 3 similar experiments.

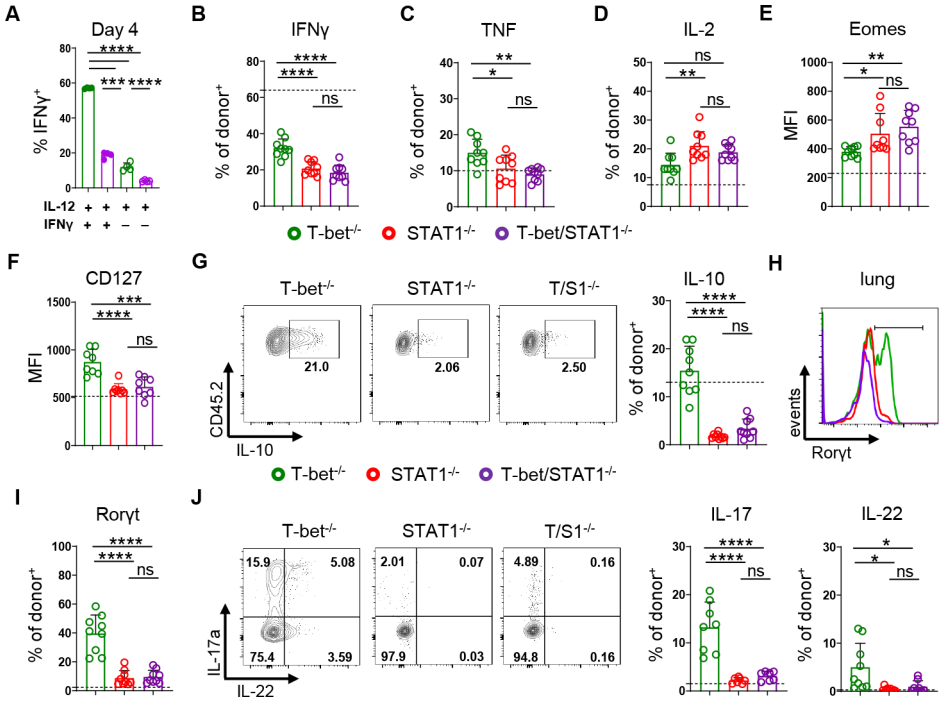

Figure 3: STAT1 regulates antiviral function in WT and T-bet$^{-/-}$ CD4 T cell responding to IAV.

(A) Naive T-bet$^{-/-}$, or T/S1$^{-/-}$ OT-II cells were cultured in triplicate wells with IFNγ and/or IL-12 as depicted for 4 days. Shown is the frequency of IFNγ^{+} cells from 3 wells per condition from 1 of 2 experiments. In separate experiments 1×10^{6} T-bet$^{-/-}$, STAT1$^{-/-}$, or T/S1$^{-/-}$ OT-II cells were transferred to congenic NK cell-depleted WT mice that were then primed with PR8-OVA$_{II}$. The frequency of donor cells in the lung at 7dpi positive for **(B)** IFNγ, **(C)** TNF, and **(D)** IL-2 is shown from individual mice, as is **(E)** donor cell expression of Eomes and of **(F)** CD127. **(G)** Representative staining and summary analysis of donor cell IL-10 production. **(H)** Representative staining and **(I)** the frequency of Rorγt^{+} donor cells from individual mice. **(J)** Representative staining and the frequency of IL-17- and IL-22-producing donor cells. Results in B-J pooled from 2 separate experiments, with dotted lines representing the average value for 4 WT donor cells responding in separate NK cell-depleted mice.

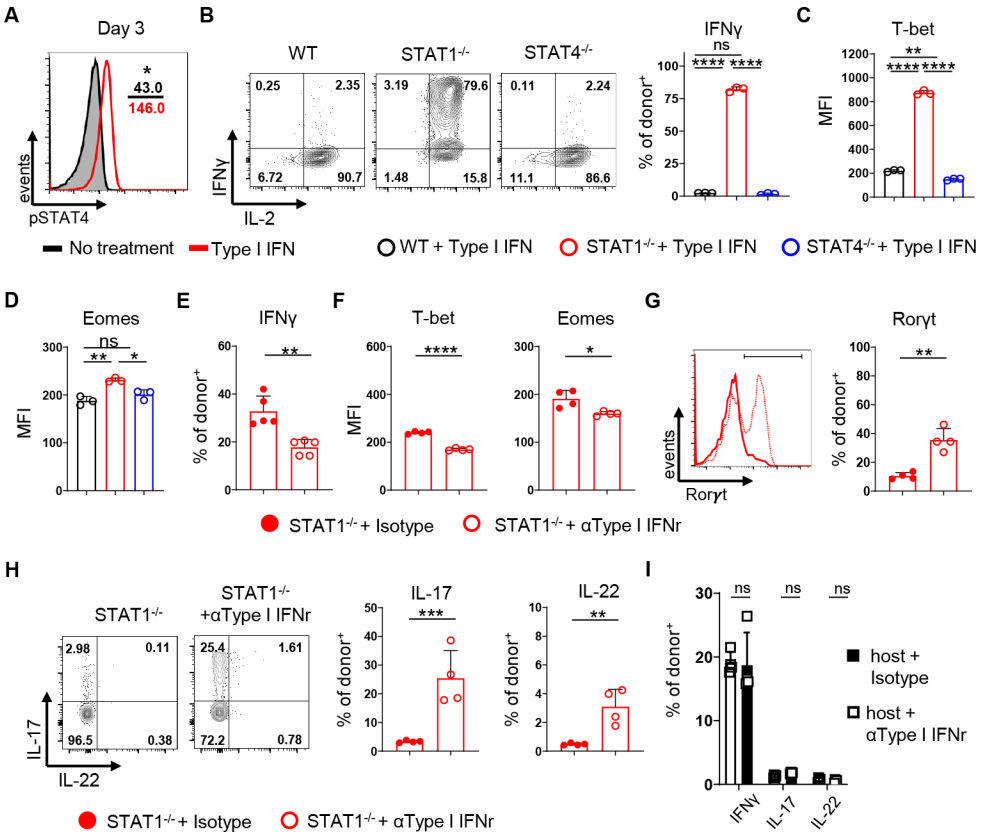

Figure 4: Type I IFN signals promote Th1 and inhibit Th17 differentiation in STAT1$^{-/-}$ CD4 T cells during IAV infection.

(A) Naive STAT1$^{-/-}$ OT-II cells were activated in Th0 conditions for 3 days then stimulated with type I IFN or not for 20 minutes and analyzed for pSTAT4. Representative staining, including control staining from STAT4$^{-/-}$ cells primed and treated in the same conditions (filled grey) with the average pSTAT4 MFI from 4 wells per condition inset. **(B)** WT, STAT1$^{-/-}$, or STAT4$^{-/-}$ OT-II cells were stimulated in Th0 conditions with type I IFN for 4 days. Representative staining for IFNγ and IL-2 and summary analysis of IFNγ production from 3 wells per condition as well as **(C)** T-bet and **(D)** Eomes expression. All results from 1 of 3 experiments. STAT1$^{-/-}$ OT-II cells were transferred to NK cell-depleted WT host mice that were primed with PR8-OVA$_{II}$ and treated with control or type I IFN receptor blocking Ab (αType I IFNr). **(E)** At 7 dpi, donor cells from individual mice were assessed for IFNγ production, **(F)** T-bet (left) and Eomes (right), **(G)** Rorγt and **(H)** production of IL-17 and IL-22. **(I)** Production of stated cytokines by host CD4+ CD44^{high} T cells in the lungs of the same mice. All results from 1 of at least 2 independent experiments.

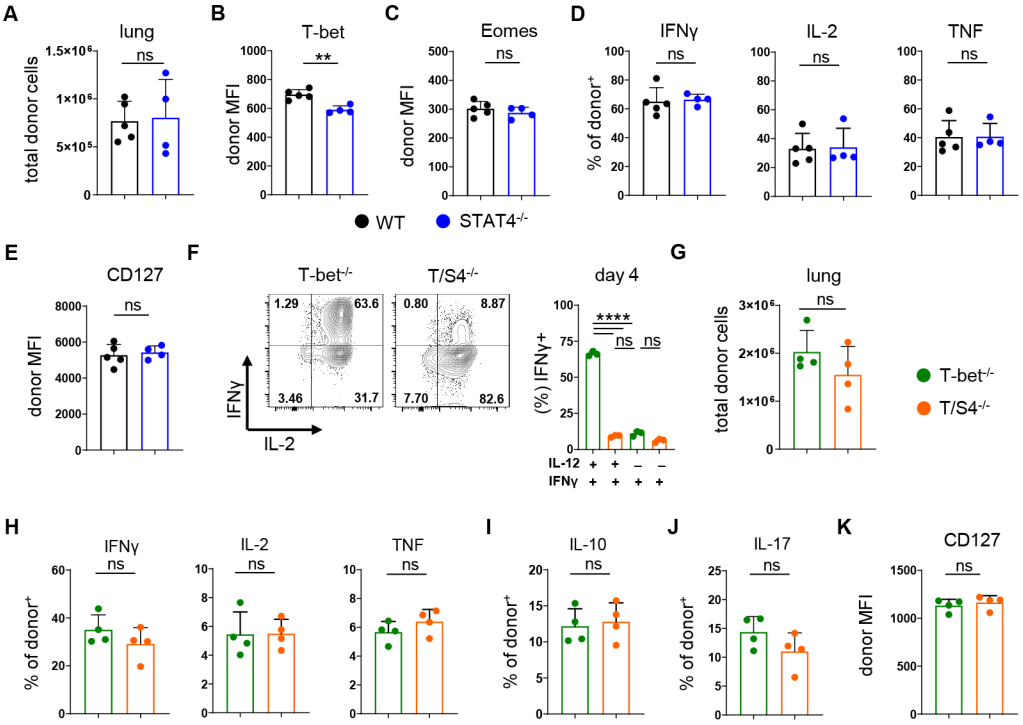

Figure 5: CD4-intrinsic STAT4 does not impact the Th1 identity of IAV-primed cells.

1×10^6 naive WT or STAT4$^{-/-}$ OT-II cells were transferred to congenic WT hosts that were challenged with PR8-OVA$_{II}$. Shown is **(A)** The number of donor cells in the lungs at 7 dpi, their MFI of **(B)** T-bet and **(C)** Eomes expression, **(D)** the frequency of IFNγ^+, IL-2$^+$, and TNF$^+$ donor cells after restimulation, and **(E)** their MFI of CD127 expression. **(F)** Naive T-bet$^{-/-}$ or T/S4$^{-/-}$ OT-II cells were cultured with IFNγ and IL-12 for 4 days with representative staining of IFNγ and IL-2 production after restimulation and summary for IFNγ^+ cells from individual wells plated in the stated conditions. Results from 1 of 2 independent experiments. In separate experiments, 1×10^6 T-bet$^{-/-}$ or T/S4$^{-/-}$ OT-II cells were transferred to separate congenic hosts and were analyzed at 7 dpi with PR8-OVA$_{II}$. Shown is **(G)** the number of donor cells in the lungs, **(H)** their production of IFNγ, TNF, and IL-2, **(I)** IL-10 and **(J)** IL-17 and **(K)** their expression of CD127. Results representative of individual mice from 1 of 3 experiments.

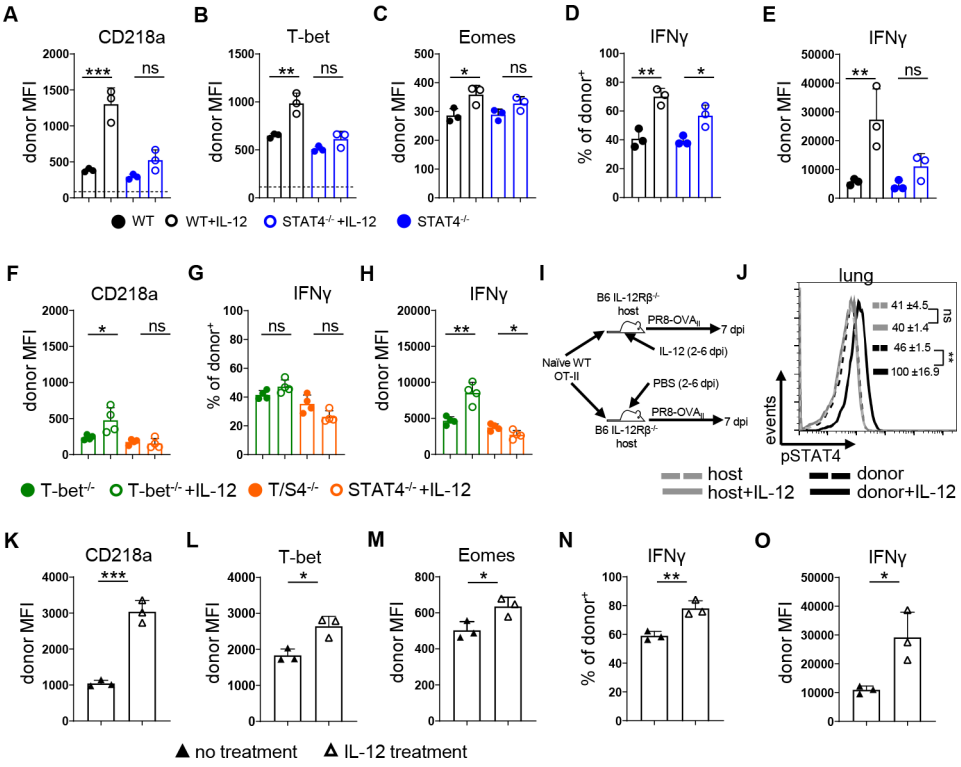

Figure 6: STAT4-dependent IL-12 signals can enhance Th1 identity during IAV infection.

WT or STAT4$^{-/-}$ OT-II cells were transferred to congenic WT hosts that were then challenged with PR8-OVA$_{II}$. Groups of mice were treated i.p. with IL-12 or PBS alone. Shown is **(A)** MFI of CD218a **(B)** T-bet and **(C)** Eomes expression by lung donor cells at 7 dpi, **(D)** the frequency of donor cells producing IFNγ and **(E)** the MFI of IFNγ^+ cells. Results from individual mice from 1 of 3 experiments. WT host mice received T-bet$^{-/-}$ or T/S4$^{-/-}$ donor cells and were treated with PBS or IL-12. Shown is donor cell **(F)** CD218a expression, **(G)** the frequency of and the **(H)** MFI of IFNγ^+ cells. Results from 1 of 2 independent experiments. **(I)** WT OT-II cells were transferred to IL-12R$\beta^{-/-}$ host mice that were infected with PR8-OVA$_{II}$ and treated with PBS or IL-12. Shown is **(J)** representative pSTAT4 staining of host CD44^{high} CD4 T cells and donor cells in the lungs at 7 dpi, with summary MFI analysis from 3 mice per group inset, **(K)** the MFI of donor cell CD218a, **(L)** T-bet, **(M)** Eomes, and **(N)** the frequency and **(O)** MFI of IFNγ^+ cells. Results from 1 of 2 experiments.

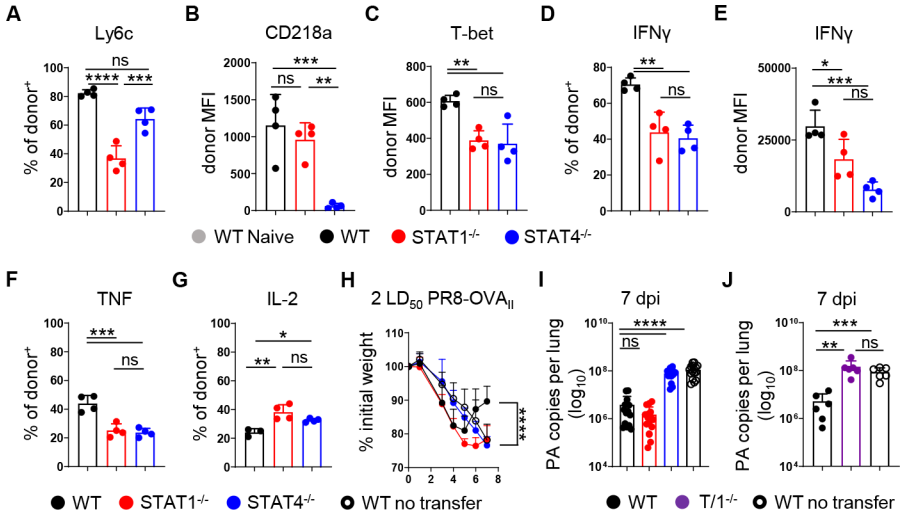

Figure 7: STAT4 activation enhances the protective capacity of Th1-primed effector cells against IAV.

WT, STAT1$^{-/-}$, or STAT4$^{-/-}$ OT-II cells were cultured in Th1 conditions as in Figure 1 and 3×10^6 of the resulting effector cells were transferred to unprimed congenic WT mice that were depleted of NK cells and then challenged with 2 LD_{50} of PR8-OVA_{II}. At 4 dpi donors in the lungs of individual mice were analyzed for **(A)** Ly6C^{high} cells, and the MFI of **(B)** CD218a and **(C)** T-bet, with **(D)** the frequency and **(E)** the MFI of IFNγ^+ cells, and the frequency of **(F)** TNF$^+$, and **(G)** IL-2$^+$ cells. Results from one of 2 experiments. Mice receiving WT, STAT1$^{-/-}$ or STAT4$^{-/-}$effectors primed in Th1 conditions, or control mice not receiving cell transfer, were analyzed for **(H)** weight loss and recovery through 7 dpi and **(I)** Pulmonary viral copies at 7 dpi. 16 mice per group; summary of 2 individual experiments. NK-cell-depleted mice receiving no transfer, or 3×10^6 WT, or T/S1$^{-/-}$ effectors primed in Th1 conditions were analyzed for viral copies at 7dpi with 2 LD_{50} PR8-OVA_{II} (6 mice per group; 1 of 2 experiments).